Supporting Information

Temperature dependent separation of metallic and semiconducting carbon nanotubes using gel agarose chromatography

I. Yahya[1‡], F. Bonaccorso[2,3], S. Clowes[1], A. C. Ferrari[2], S. R. P. Silva[1*].

[1] Advanced Technology Institute, University of Surrey, Guildford GU2 7XH, UK

[2] Cambridge Graphene Centre, Cambridge University, Cambridge CB3 0FA, UK

[3] Istituto Italiano di Tecnologia, Graphene Labs, 16163 Genova, Italy

[‡] Currently at the Department of Electrical, Electronic and Systems Engineering, Faculty of Engineering and Built Environment, Universiti Kebangsaan Malaysia, 43600, Malaysia

* Corresponding author email: s.silva@surrey.ac.uk

1. <u>**Raman spectra for DIPS-CNTs**</u>

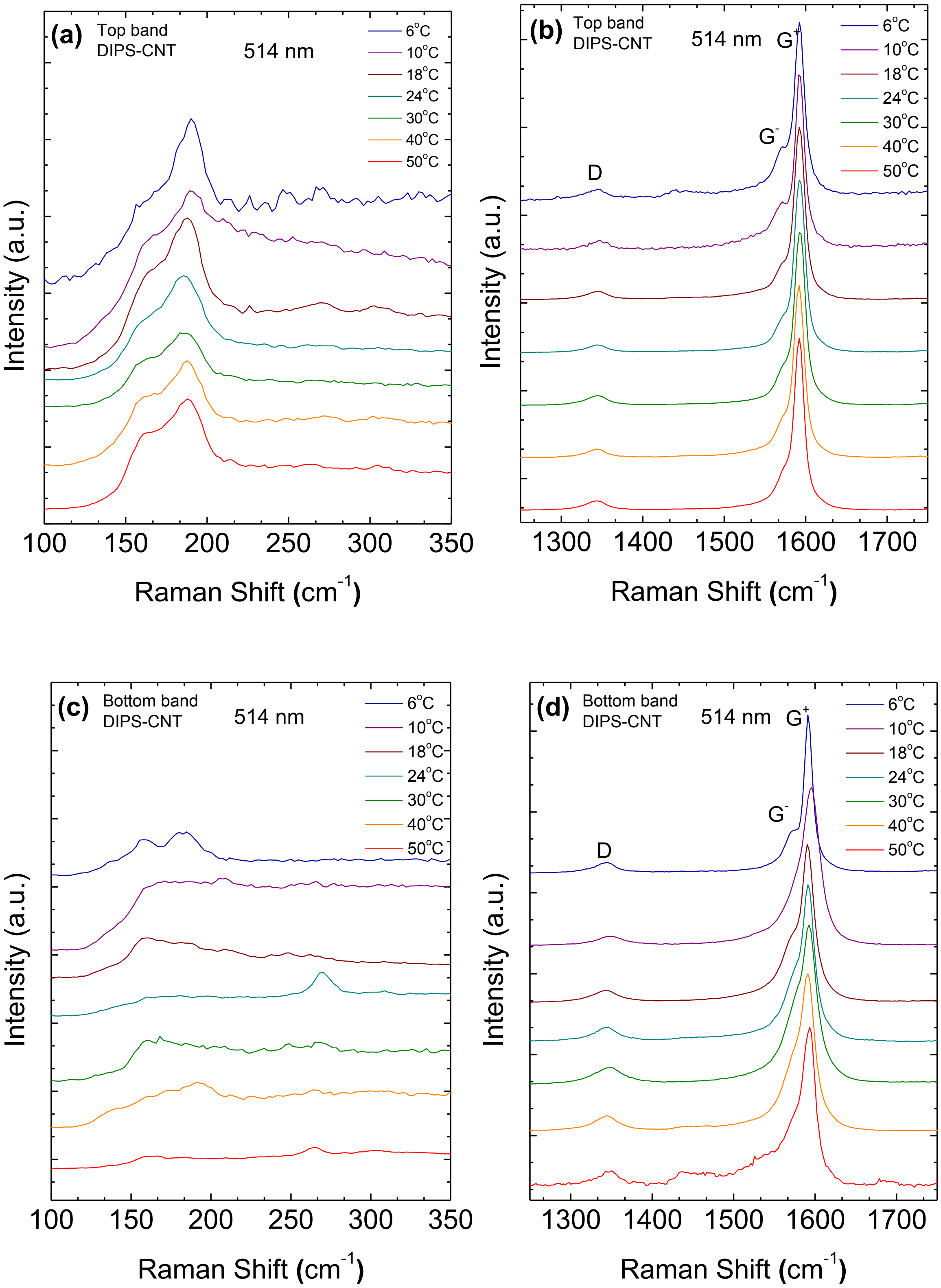

Fig. S1.1: Raman spectra of DIPS-CNTs separated at different temperatures; excitation wavelength 514 nm. (a) RBM and (b) D-G regions for top band; (c) RBM and (d) D-G regions for bottom band.

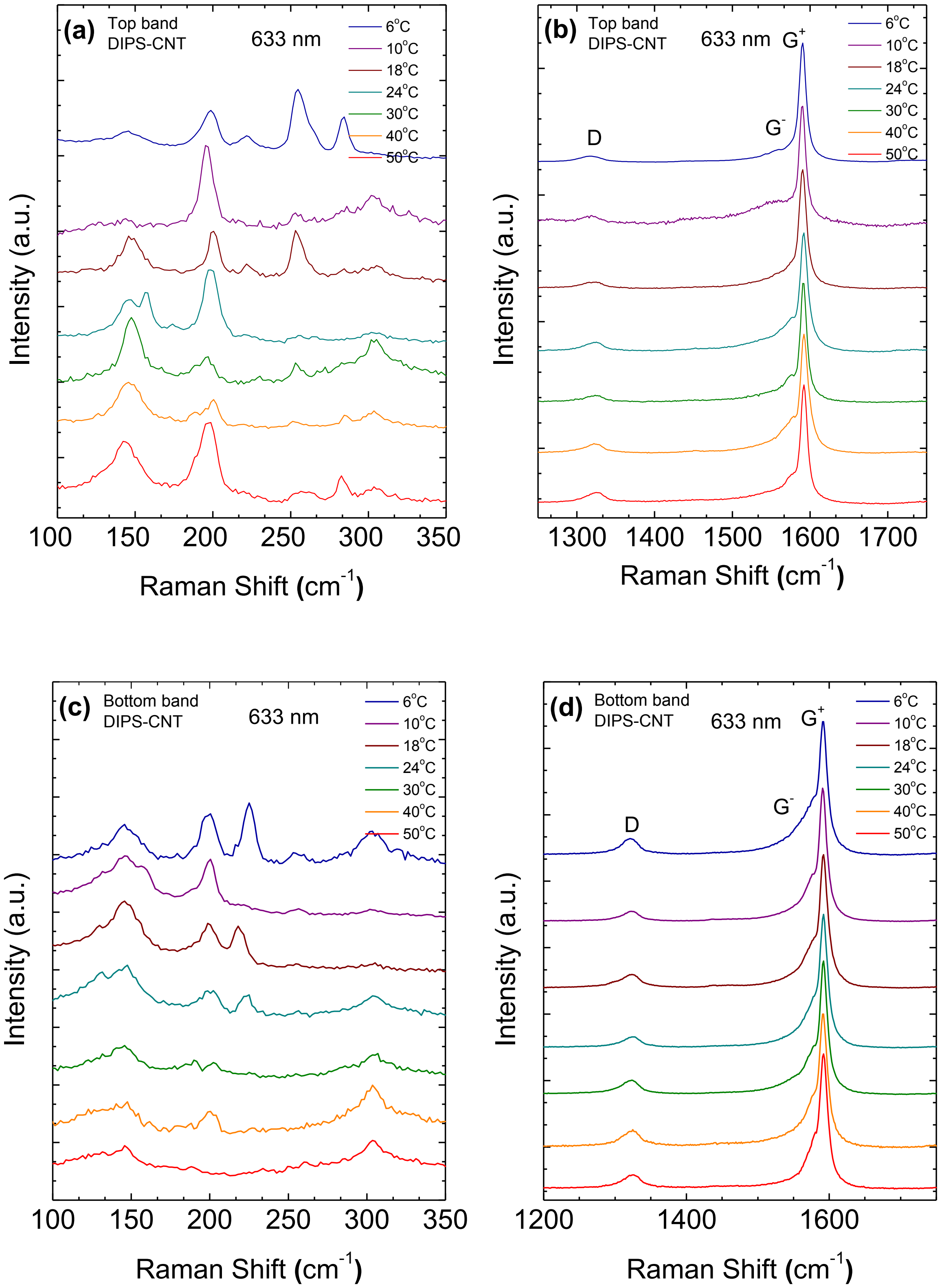

Fig. S1.2: Raman spectra of DIPS-CNTs separated at different temperatures; excitation wavelength 633 nm. (a) RBM and (b) D-G regions for top band; (c) RBM and (d) D-G regions for bottom band.

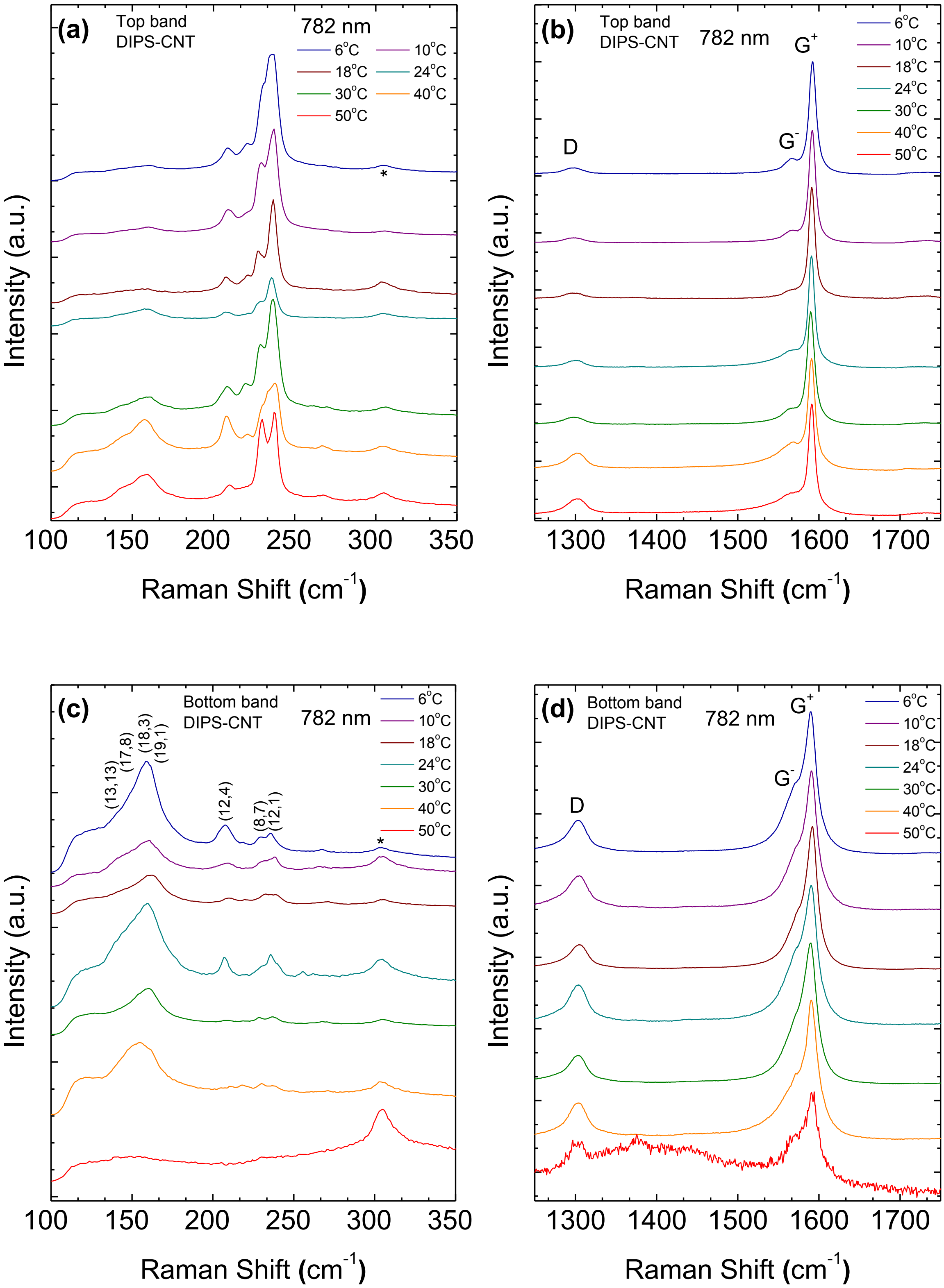

Fig. S1.3: Raman spectra of DIPS-CNTs separated at different temperatures; excitation wavelength 782 nm. (a) RBM and (b) D-G regions for top band; (c) RBM and (d) D-G regions for bottom band.

2. **<u>Raman spectra for AD-CNTs</u>**

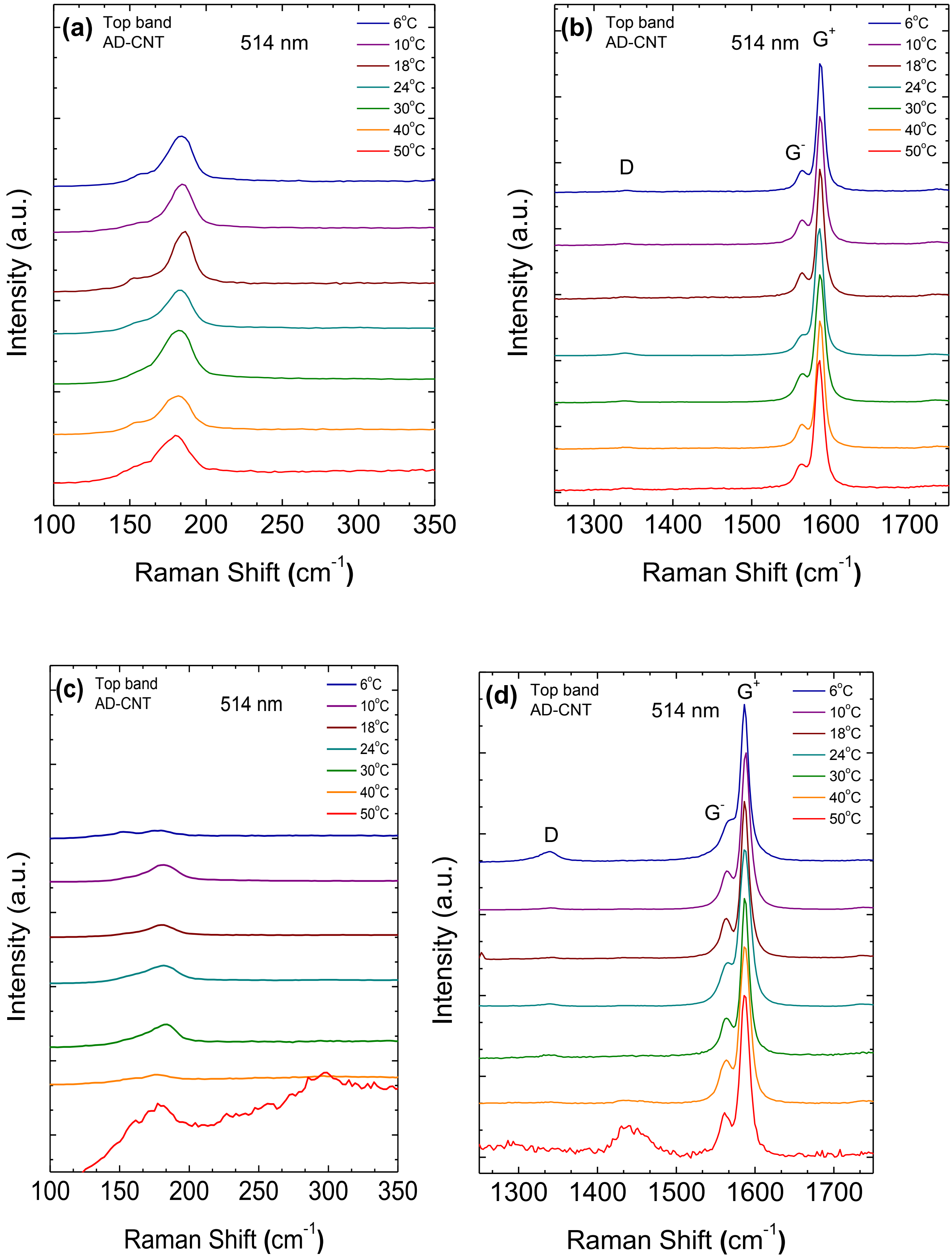

Figure S2.1: Raman spectra of AD-CNTs separated at different temperatures; excitation wavelength 514 nm. (a) RBM and (b) D-G regions for top band; (c) RBM and (d) D-G regions for bottom band.

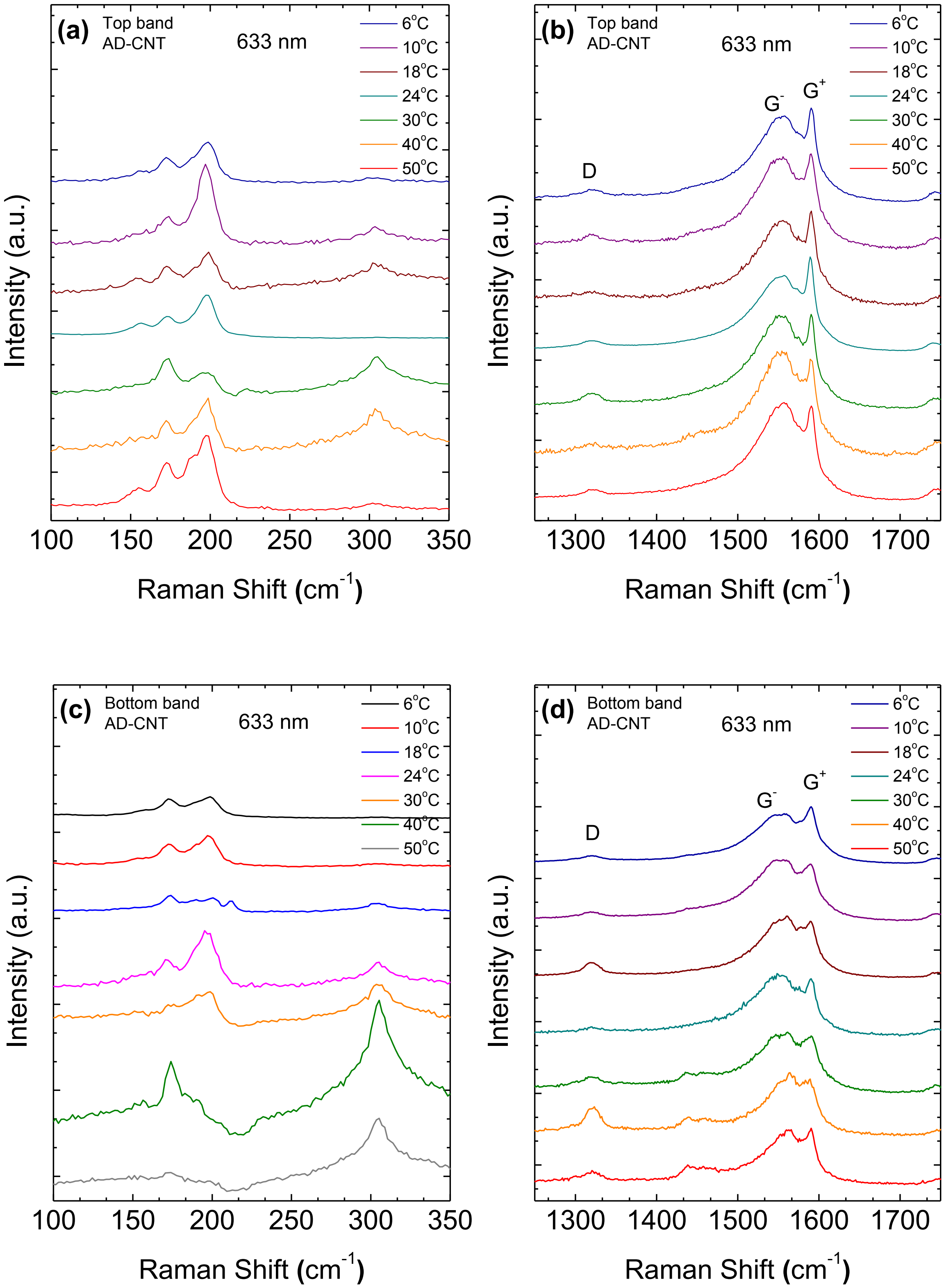

Fig. S2.2: Raman spectra of AD-CNTs separated at different temperatures; excitation wavelength 633 nm. (a) RBM and (b) D-G regions for top band; (c) RBM and (d) D-G regions for bottom band.

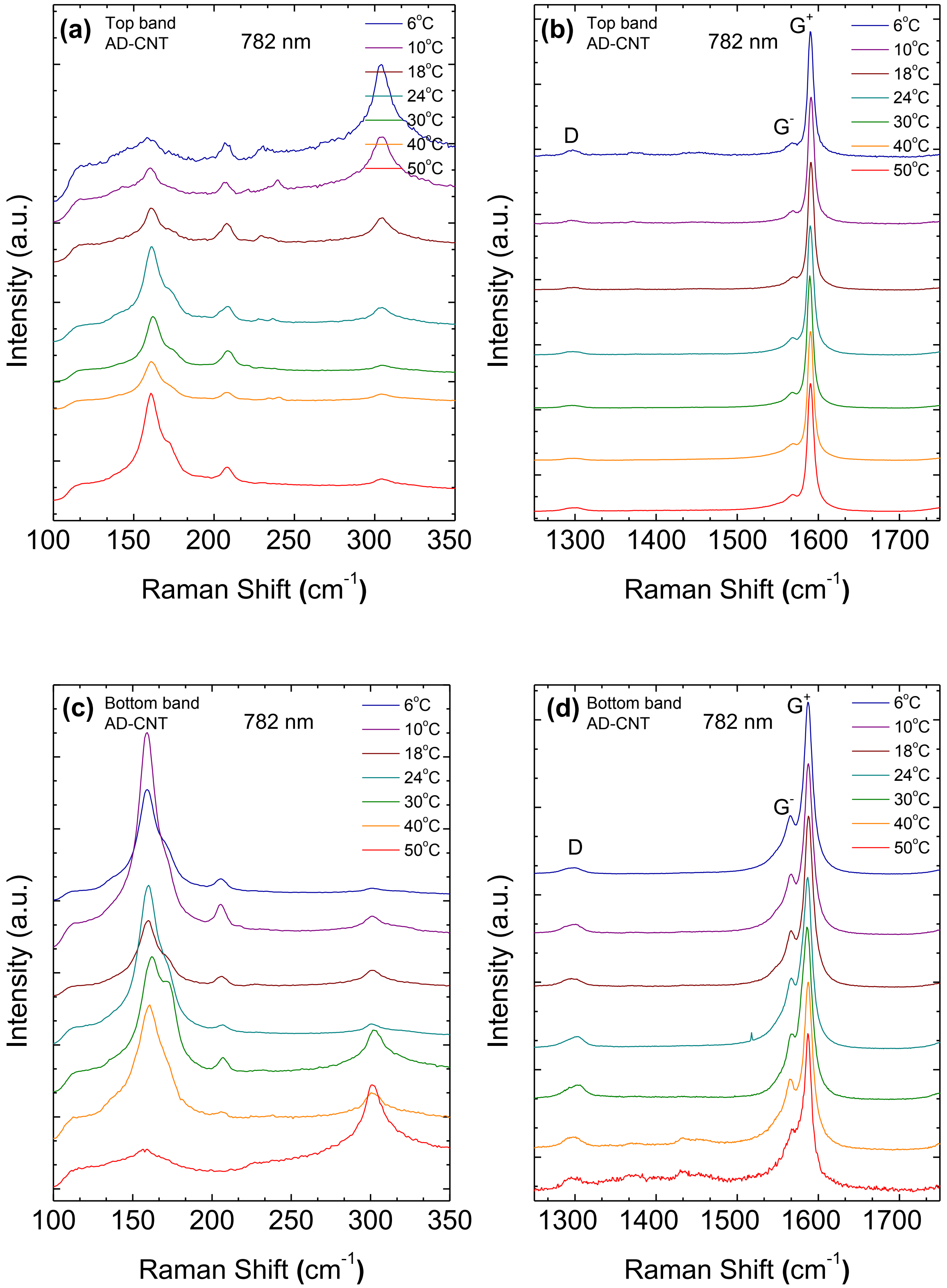

Fig. S2.3: Raman spectra of AD-CNTs separated at different temperatures; excitation wavelength 782 nm. (a) RBM and (b) D-G regions for top band; (c) RBM and (d) D-G regions for bottom band.

3. Raman spectra of HiPco-SWNTs

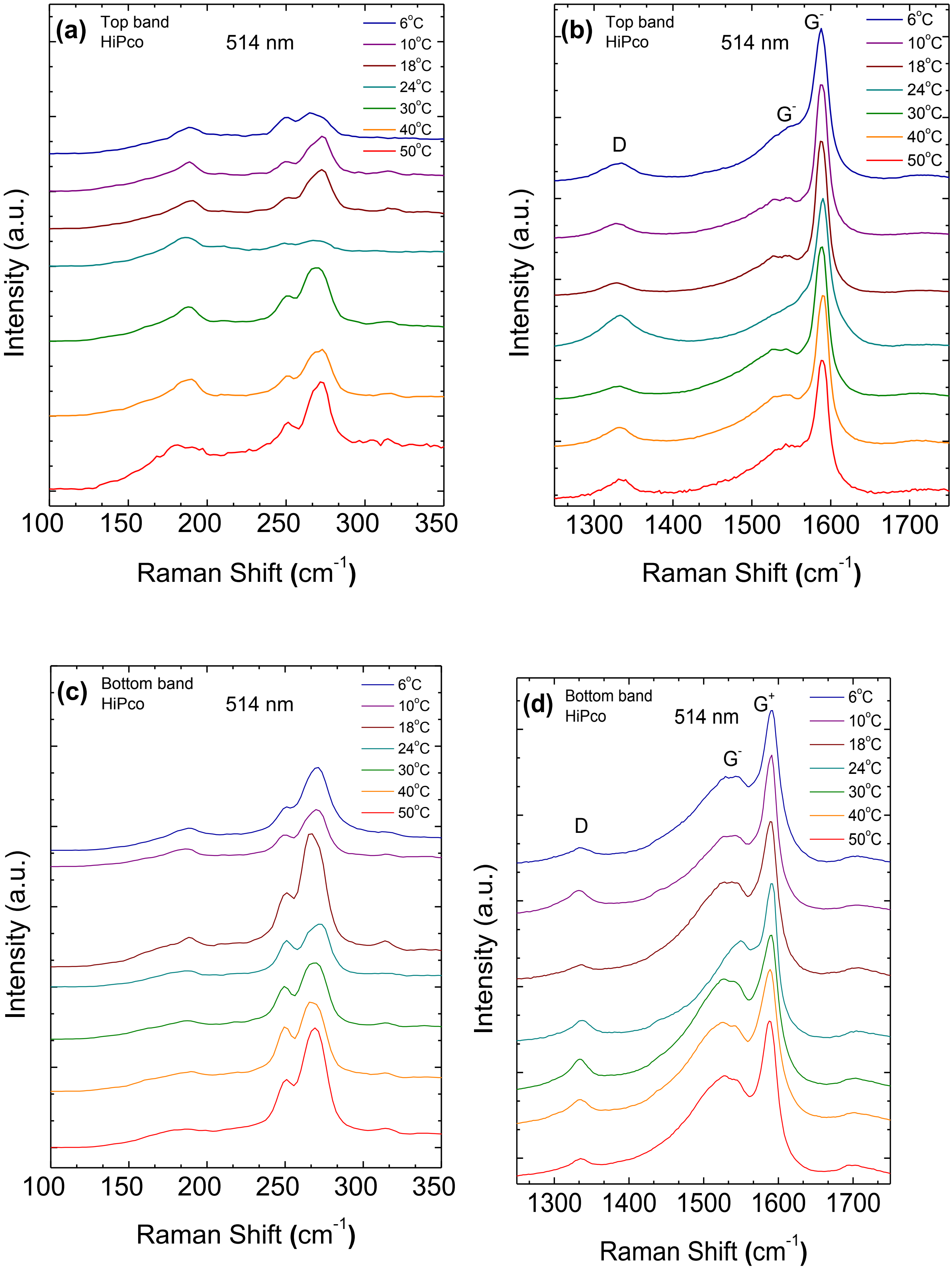

Fig. S3.1: Raman spectra of sample HiPco separated at different temperatures; excitation wavelength 514 nm. (a) RBM and (b) D-G regions for top band; (c) RBM and (d) D-G regions for bottom band.

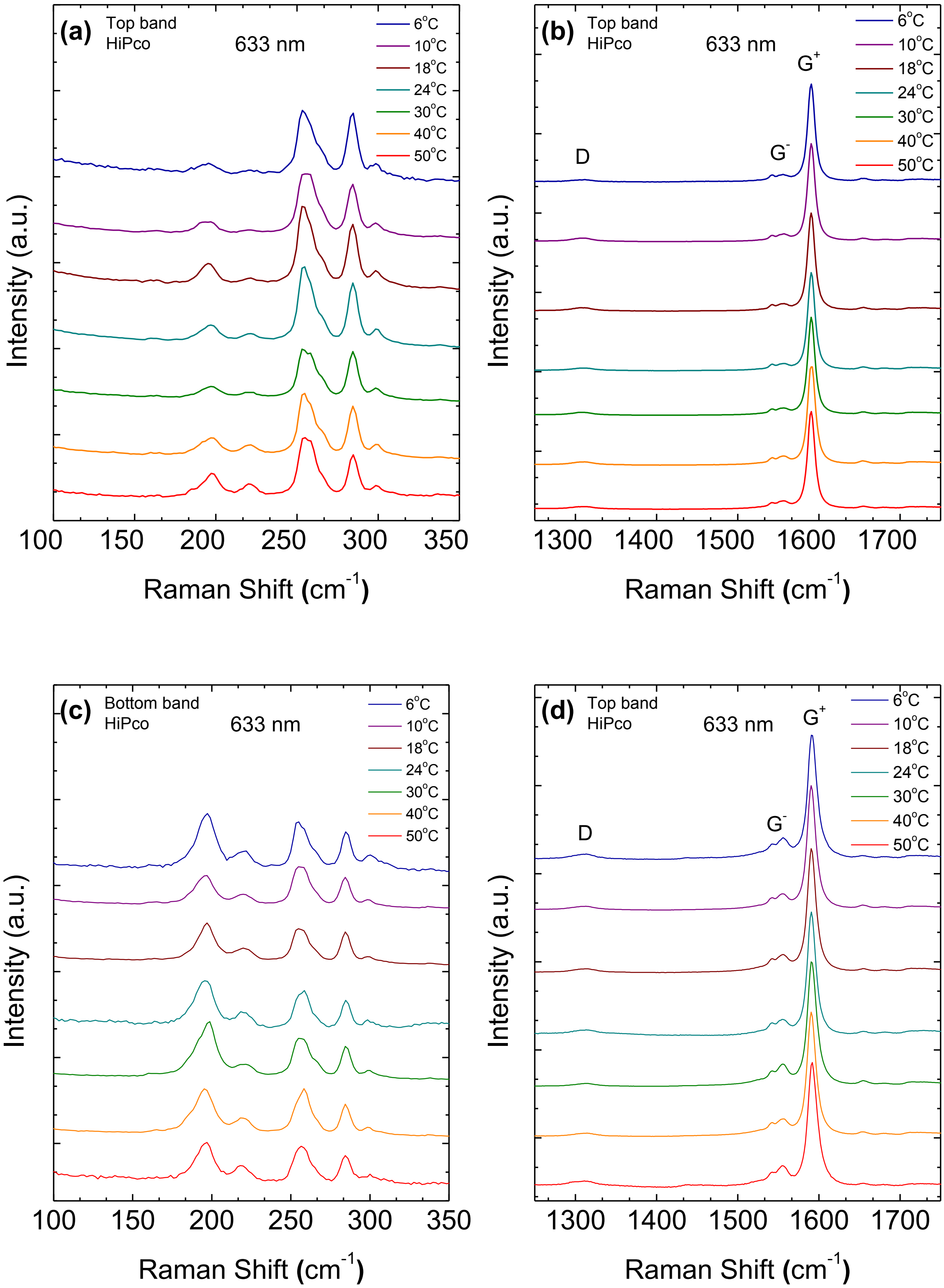

Fig. S3.2: Raman spectra of HiPco-SWNTs separated at different temperatures; excitation wavelength 633 nm. (a) RBM and (b) D-G regions for top band; (c) RBM and (d) D-G regions for bottom band.

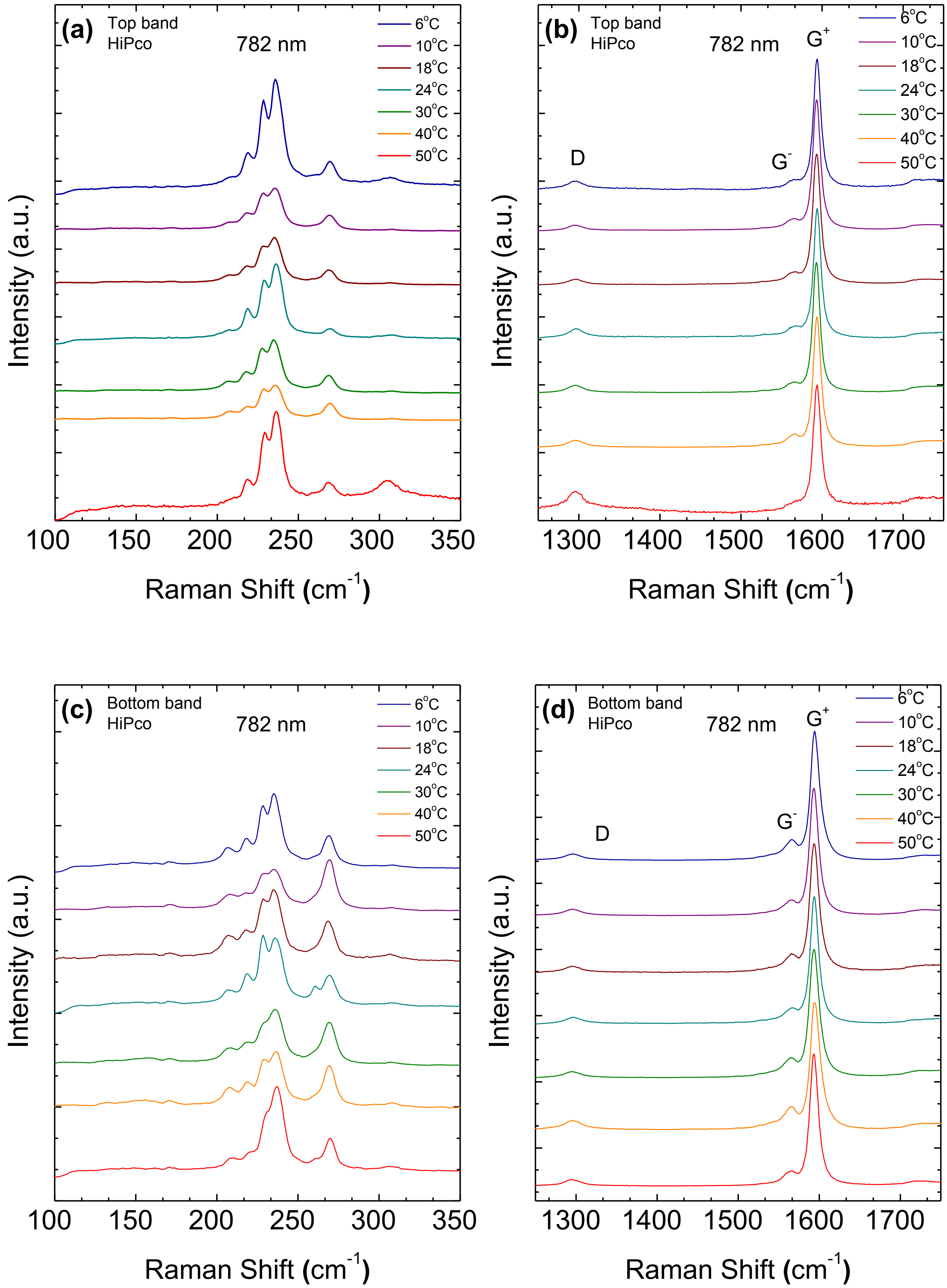

Fig. S3.3: Raman spectra of HiPco-SWNTs separated at different temperatures; excitation wavelength 782 nm. (a) RBM and (b) D-G regions for top band; (c) RBM and (d) D-G regions for bottom band.

4. Raman spectra of CoMoCAT-SWNTs

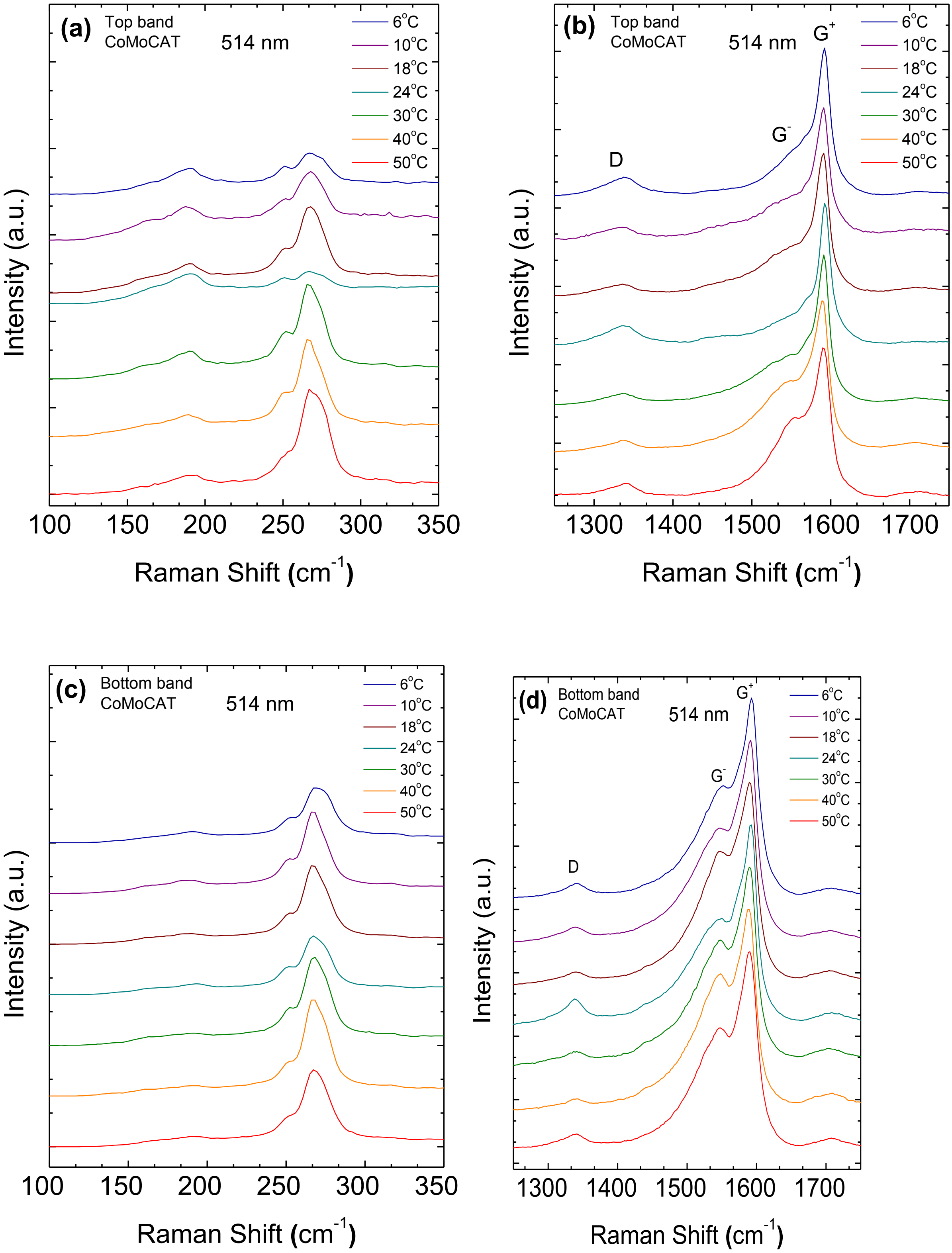

Fig. S4.1: Raman spectra of CoMoCAT-SWNTs separated at different temperatures; excitation wavelength 514 nm. (a) RBM and (b) D-G regions for top band; (c) RBM and (d) D-G regions for bottom band.

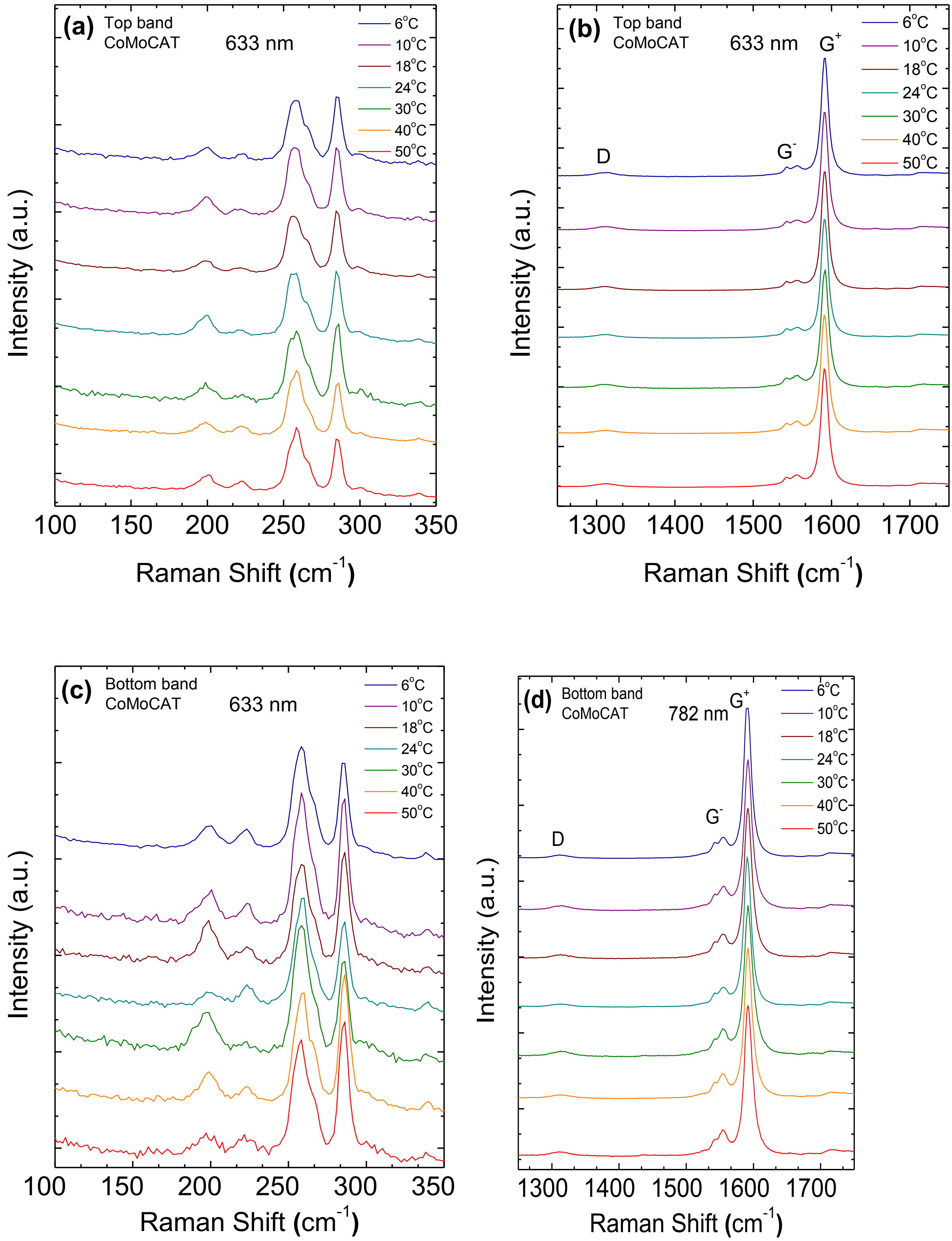

Fig. S4.2: Raman spectra of CoMoCAT-SWNTs separated at different temperatures; excitation wavelength 633 nm. (a) RBM and (b) D-G regions for top band; (c) RBM and (d) D-G regions for bottom band.

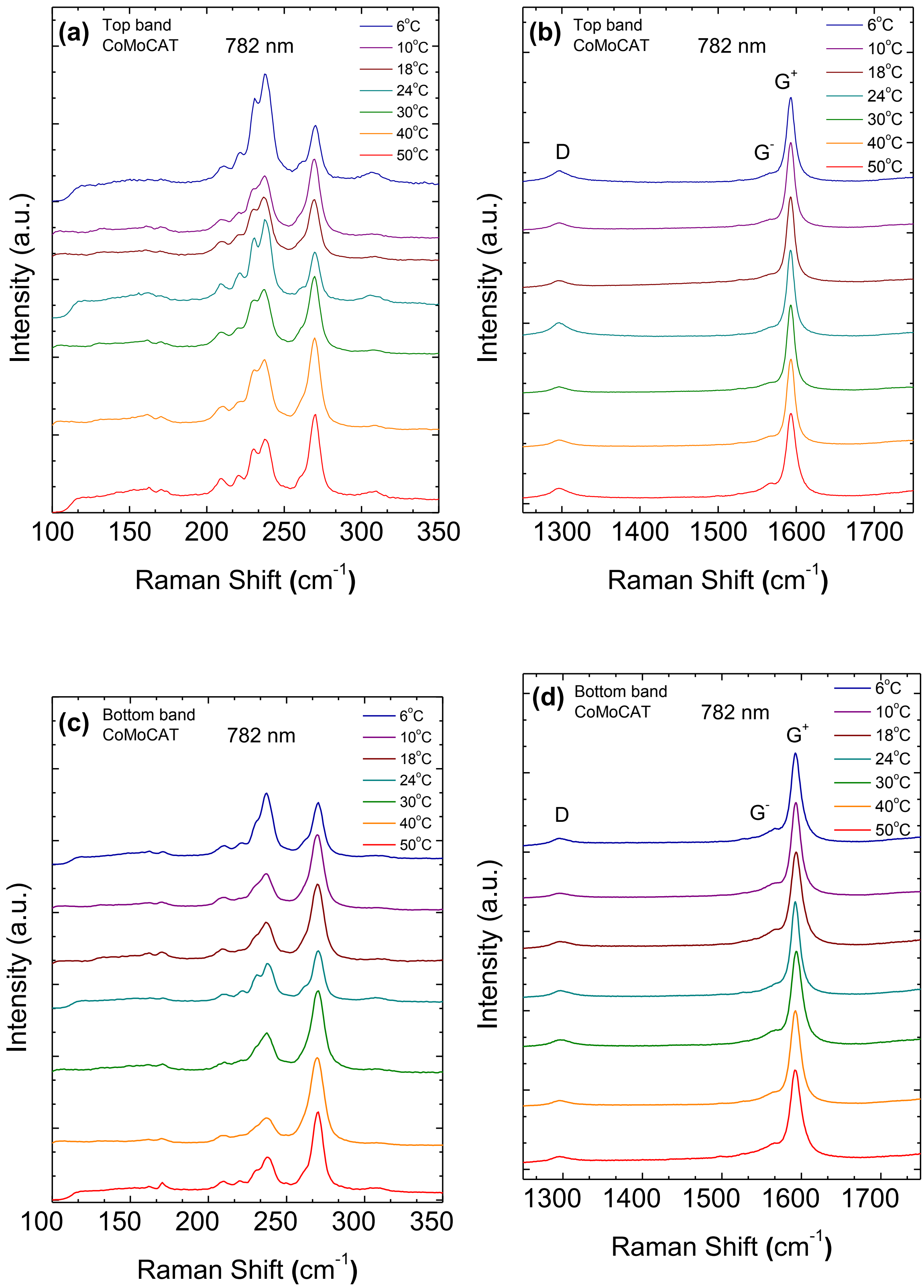

Fig. S4.3: Raman spectra of CoMoCAT-SWNTs separated at different temperatures; excitation wavelength 782 nm. (a) RBM and (b) D-G regions for top band; (c) RBM and (d) D-G regions for bottom band.

5. Relative SWNT concentrations in the top and bottom bands after separation

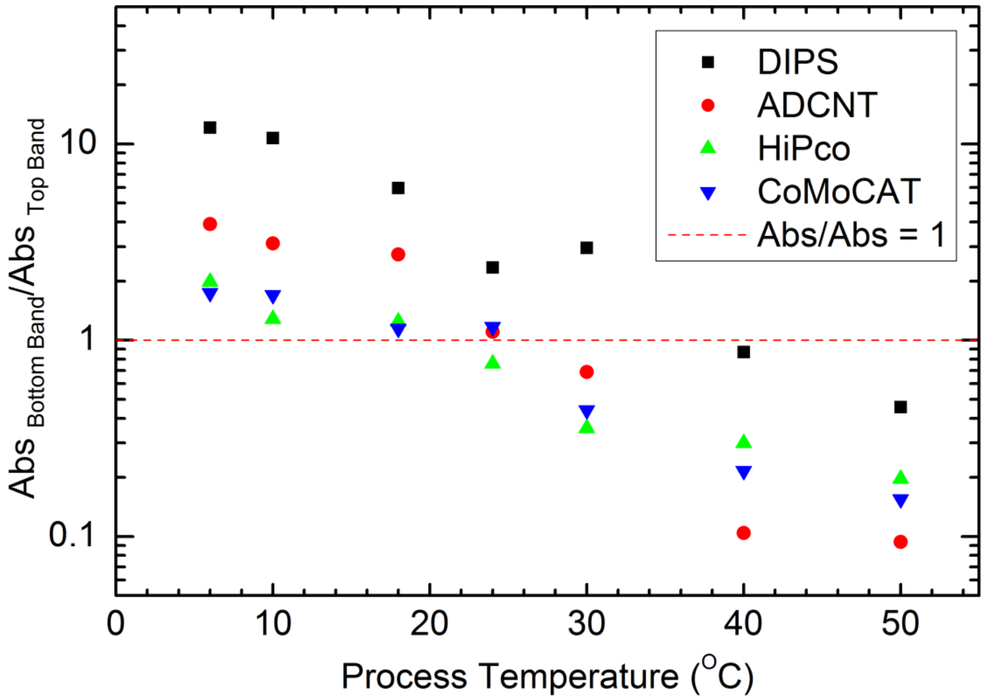

Fig. S5: Ratio of optical absorption of the bottom band to the top band as a function of process temperature. The optical absorption is directly proportional to the SWNT concentration in the respective bands.

Fig. S5 reports the variation of the optical absorption with respect to temperature for each sample at wavelengths corresponding to the optical transition boundaries, i.e. between the excitonic transitions. The absorbance at these wavelengths is the background contribution due to the carbon π-plasmon, which is directly proportional to the SWNT concentration.